Theoretical reconsideration of antiferromagnetic Fermi surfaces in URu$_2$Su$_2$

To cite this article: Hiroshi Yamagami 2011 *J. Phys.: Conf. Ser.* **273** 012064

View the article online for updates and enhancements.

Theoretical reconsideration of antiferromagnetic Fermi surfaces in URu_2Su_2

Hiroshi Yamagami

Department of Physics, Faculty of Science, Kyoto Sangyo University, Kyoto 603-8555, Japan

E-mail: `yamagami@cc.kyoto-su.ac.jp`

Abstract. In an itinerant $5f$-band model, the antiferromagnetic (AFM) Fermi surfaces of URu_2Si_2 are reconsidered using a relativistic LAPW method within a local spin-density approximation, especially taking into account the lattice parameters dependent on pressures. The reduction of the z-coordinate of the Si sites results in the effect of flattening the Ru-Si layers of URu_2Si_2 crystal structure, thus weakening a hybridization/mixing between the U-$5f$ and Ru-$4d$ states in the band structure. Consequently the $5f$ bands around the Fermi level are more flat in the dispersion with decreasing the z-coordinate, thus producing three closed Fermi surfaces like "curing-stone", "rugby-ball " and "ball". The origins of de Haas-van Alphen branches can be qualitatively interpreted from the obtained AFM Fermi surfaces.

1. Introduction

In highly-correlated-electron system, the " hidden order " (HO) parameter of URu_2Si_2 at T_o = 17.5 K is one of reminding issues we have not yet shared a common view [1]: The bulk experiments of specific heat and Hall effect indicate that a large energy gap opens at the Fermi level (E_F), thus releasing most of the carriers below T_o [2]. Under the pressure the HO state with a tiny magnetic moment changes into a large moment antiferromagnetic (AFM) state at P_c=15 kbar [3]. However, de Haas-van Alphen (dHvA) measurements provide very limited information concerning the Fermi surface [4], and theoretically it is still hard to give a consistent understanding of the U-$5f$ states, not only in the band structure and Fermi surface, but also in the paramagnetic (PM) and ordered states [4, 5, 6].

At ambient pressure, URu_2Si_2 crystallizes in the tetragonal $ThCr_2Si_2$ crystal structure (space group $I4/mmm$) with the lattice constants $a = 4.1239$Å and $c = 9.5817$Å [7] and the z-coordinate of the Si sites $z = 0.371$ [8]. The ambient pressure lattice symmetry and crystal structure persist in the PM, HO and AFM phases. With increasing pressures, both the a- and c-axes reduce with the c-axis contracting slightly more than the a-axis, and additionally the z-coordinate decrease with applied pressures. At 27 kbar, the lattice parameters of the AFM phase are measured as $a = 4.109$Å , $c = 9.515$Å and $z = 0.356$ [9]. The reduction of z-coordinate is expected to control a c-f hybridization, thus resulting in a flattening of the $5f$ bands and a distortion of the Fermi surface volume.

Recently itinerant $5f$ bands of URu_2Si_2 around E_F was directly detected in the PM phase using soft x-ray angle-resolved photoemission spectroscopy (SXARPES) [10], and the AFM Fermi surfaces are closely related to the HO Fermi surfaces in the dHvA measurements under the pressure [11]. In an itinerant $5f$-based model, therefore, we need to reconsider the PM and
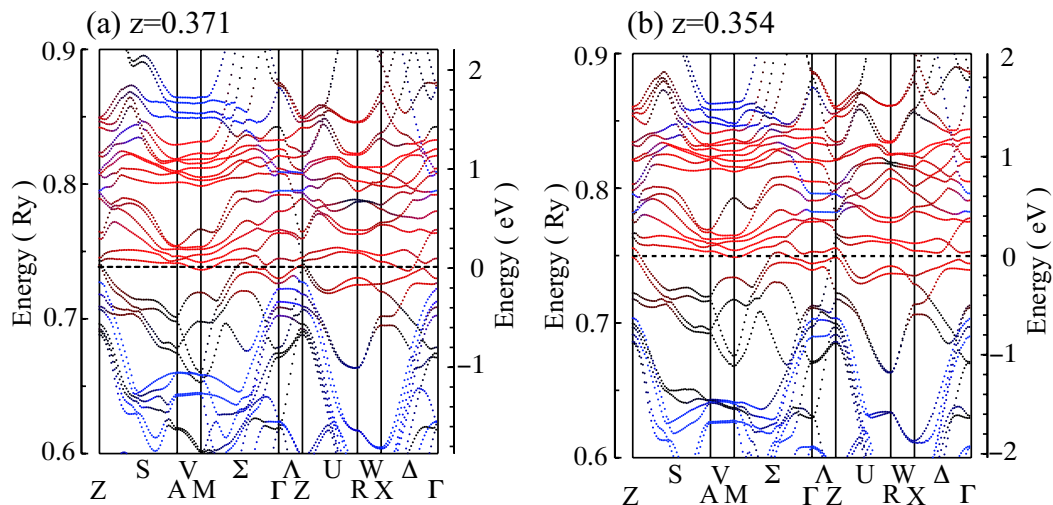
Figure 1. AFM band structures of URu$_2$Si$_2$ calculated with two z-parameters of (a) $z = 0.371$ and (b) $z = 0.354$.

AFM electronic structure theoretically. Taking into account the lattice parameters dependent on pressures [9], here, the AFM Fermi surface calculations are performed using the same relativistic LAPW (RLAPW) method [12] within a local spin-density approximation (LSDA) [13] as previously used to obtain the PM [4] and the AFM Fermi surfaces [14].

The RLAPW method is based on the spin-polarized coupled Dirac equation (SPCDE) in the LSDA. The AFM configuration is set by orienting the spin and orbital directions at each site with use of local rotation matrix. The densities and potentials are constructed in the muffin-tin approximation. In the iterative process, all-electron calculations are carried out; the $5f^3$, $6p^6$, $6d^1$ and $7s^2$ states at the U site, $4d^7$ and $5s^1$ at the Ru sites, and $3s^2$ and $3p^2$ at the Si sites are treated as valence electrons, while the other electrons are solved by SPCDE under atomic-like boundaries at each site.

2. Band structure of AFM phase dependent on z coordinate

Figure 1 shows the z-parameter dependence of the AFM band structures of URu$_2$Si$_2$ in the vicinity of E_{F}, which is indicated by the horizontal broken line. In Fig. 1(a) the AFM band structure calculated with $z = 0.371$ at ambient pressure, of which the z-parameter was used to create the previous AFM Fermi surfaces [14], is shown along the simple-tetragonal symmetry axes of the AFM Brillouin zone. The AFM band structure with $z = 0.354$ of the AFM phase at 27 kbar [9] is illustrated in Fig. 1(b). The U-$5f$ and the Ru-$4d$ components for each of the bands are expressed by a relative ratio from red ($5f$) to blue ($4d$) colors. The main differences of the two band structures are as follows: First, the top of the Ru-$4d$ (blue) bands of $z = 0.354$ (Fig. 1(b)) shifts lower down from E_{F} than that of $z = 0.371$ (Fig. 1(a)) with narrowing the bandwidth, and thus the hybridization between the U-$5f$ and the Ru-$4d$ states becomes much weaker. Secondly, the U-$5f$ (red) bands just around E_{F} along the Σ and Δ axis are partially more flattened with decreasing the z-parameter, and especially we can see that a gap opens along the Δ axis.

3. Fermi surfaces of AFM phase and de Haas-van Alphen frequencies

As seen in Fig.1, two bands indexed as band36 and band37 keep crossing E_{F} in both the band structures to make up the Fermi surfaces, where the band index is determined by numbering

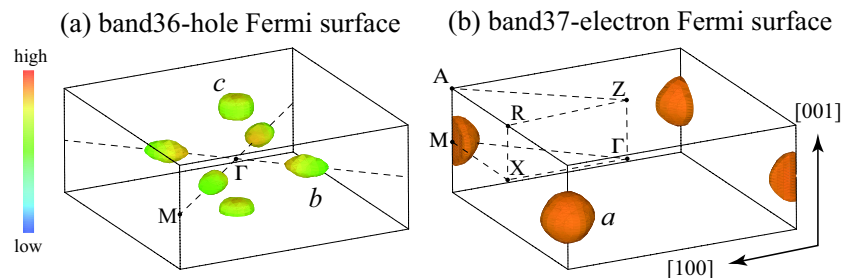(a) band36-hole Fermi surface   (b) band37-electron Fermi surface

Figure 2. (a) Hole Fermi surface for band36 and (b) electron Fermi surface of band37 obtained from AFM band structure of $z = 0.354$ in URu_2Si_2.

from the bottom of the valence bands. A few small parts of the previous Fermi surfaces [14], however, vanish for the cause of changing the band dispersions around E_F. Figures 2(a) and (b) show the hole Fermi surface of the band36 and electron Fermi surface of the band37, respectively, which are obtained from the AFM band structure of $z = 0.354$ in Fig. 1(b). The hole Fermi surfaces are composed of a "curling-stone"-shaped part around the Z point and four "rugby-ball"-like parts along the Γ-M (Σ) axis. On the other hand the electron Fermi surface is formed from a big "ball" centered at the M point, of which the volume is equal to that of all the hole Fermi surfaces because of the electron number being even in URu_2Si_2. Accordingly it can be said that the AFM electronic state of URu_2Si_2 is a semi-metallic with the small electron and hole carriers. The electronic specific heat coefficient γ is estimated as 1.45 mJ/(K²·mole) from the total density of states.

The color expression of Fig. 2 shows the intensity of $5f$ contribution on the Fermi surfaces according to a color indicator, where the highest contribution is red and the opposite is blue. As understood from the colors on the Fermi surfaces, all the hole Fermi surfaces have an anisotropic $5f$ distribution orienting higher near the Γ point, while the electron Fermi surface are constructed from almost pure $5f$ bands. Generally the intensity of the $5f$ states on the Fermi surfaces has a certain amount of relationship with a size of local band gradient around E_F, or the cyclotron effective mass (CEM) in any direction. Therefore the CEM of the curling-stone and rugby-ball Fermi surfaces behaves as a monotonically decreasing function with respect to the field angles from the [001] to the [100] directions, while the big-ball CEM is large with a small angular dependence.

In Fig. 3 we show the angular dependence of dHvA frequencies obtained from the big ball, the rugby-ball and the curling-stone Fermi surfaces, corresponding to theoretical branches a, b and c, respectively. For comparison, the experimental dHvA frequencies measured in the HO phase are depicted by open circles [4], since the dHvA frequencies of the AFM phase are similar to those of the HO phase. Although there appear quantitative differences between the theoretical and the experimental branches, it can be suggested that the α, β and γ branches are derived from the big ball, the rugby-ball and the curling-stone Fermi surfaces, respectively. Moreover it should be emphasized that the theoretical branches a, b and c remain even in changing the lattice parameters.

4. Discussion and conclusion

Under pressures the reduction of the z-parameter results in the effect of flattening the Ru-Si layers of URu_2Si_2 crystal structure [9]. In the band structure the dispersion of the $5f$ bands around E_F gets more flat, because the hybridization/mixing between the U-$5f$ and Ru-$4d$ states becomes weaker. From the AFM calculations with $z = 0.354$, it is found out that the local spin moment at the U site is $-0.39\mu_B$ and the corresponding orbital moment is $0.93\mu_B$. Therefore
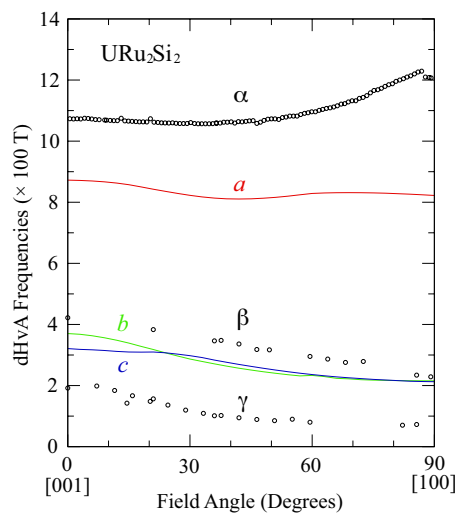
Figure 3. Angular dependence of de Haas-van Alphen frequencies from [001] to [100] directions of applied field. The theoretical branches a, b and c by colored lines originate from the big ball, the rugby-ball and the curling-stone Fermi surfaces, respectively. The observed branches α, β and γ are shown by open circles [4].

the total magnetic moment is obtained as $0.54\mu_B$ in comparable agreement with $0.4\mu_B$ of the AFM phase in neutron-scattering experiment [3]. Surprisingly, the local magnetic moment at the Ru sites is polarized with $0.36\mu_B$ in the calculation. As a next step to clarify the HO Fermi surface, we will discuss the SXARPES [10] with the PM Fermi surface calculated in the itinerant $5f$ band picture.

Acknowledgments

References

[1] Shah N, Chandra P, Coleman P and Mydosh J A 2000 *Phys. Rev.* B **61** 564
[2] Behnia K, Bel R, Kasahara Y, Nakajima Y, Jin H, Aubin H, Izawa K, Matsuda Y, Flouquet J, Haga Y, Ōnuki Y and Lejay P 2005 *Phys. Rev. Lett.* **94** 156405
[3] Amitsuka H, Sato M, Metoki N, Yokoyama M, Kuwahara K, Sakakibara T, Morimoto H, Kawarazaki S, Miyako Y and Mydosh J A 1999 *Phys. Rev. Lett.* **83** 5114
[4] Ohkuni H, Inada Y, Tokiwa Y, Sakurai K, Settai R, Honma T, Haga Y, Yamamoto E, Ōnuki Y, Yamagami H, Takahashi S and Yanagisawa S 1999 *Phil. Mag.* B **79** 1045
[5] Elgazzar S, Rusz J, Oppeneer P M and Mydosh J A 2009 *Nat. Mater.* **8** 337
[6] Haule K and Kotliar G 2009 *Nat. Phys.* **5** 796
[7] Palstra T T M, Menovsky A A, van den Berg J, Dirkmaat A J, Kes P H, Nieuwenhuys G J and Mydosh 1985 *Phys. Rev. Lett.* **55** 2727
[8] Cordier G, Czech E, Schäfer H, and Woll P 1985 *J. Less-Common Met.* **110** 327
[9] Jeffries J R, Butch N P, Hamlin J J, Sinogeikin S V, Evans W J and Maple M B 2010 *cond-mat.str-el* arXiv:1002.2245v1
[10] Kawasaki I, Fujimori S.-i, Takeda Y, Okane T, Yasui A, Saitoh Y, Yamagami H, Haga Y, Yamamoto E and Ōnuki Y. to be submitted to 2010 *J. Phys.: Conf. Series* (SCES2010)
[11] Flouquet J *private commun.*
[12] Yamagami H 2000 *Phys. Rev.* B **61** 2426
[13] von Barth U and Hedin L 1972 *J. Phys.* C **5** 1629
[14] Yamagami H and Hamada N 2000 *Physica* B **284-288** 14155